Materials Physics and Mechanics 41 (2019) 91-96 Received: January 31, 2018

EVOLUTION OF STEAM AND GAS PLUME GENERATION ON LASER TREATING OF METALS IN LIQUID

A.Yu. Ivanov*, A.V. Kapytski, S.V. Vasiliev

YankaKupalaGrodnoStateUniversity, OzheshkoStreet 22, Grodno, Belarus

*e-mail: ion_ne@mail.ru

Abstract. Evolution of steam and gas plume generation on the surface of an irradiated metal was investigated experimentally. It is shown that on using GOR-100M operating in a free oscillating regime the form of a crater developed in an irradiated target beingin water and air differs drastically.It is found that the substantial difference in the forms of crater surfaces developed is determined by different character of plasma, steam and gas mixture flow.
Keywords: fast holographic filming, laser radiation, steam and gas mixture flow

1. Introduction

The main opinions about the destruction mechanisms of solids surrounded with gas during their treatment by laser beams with the radiation flux density varied from 10^5 to 10^6W/sm^{2}are considered. The work aim is the investigation of processes running near a metal target mounted in water.

2. Experimental equipment and experimental results

The scheme of the experimental setup used in the study is presented in Fig. 1. The radiation of the GOR-100M ruby laser (*1*) (λ = 0.694 μm) operating in the free oscillation regime (pulse duration ~1.2 mc) passed through the focusing system (*2*) and was directed onto the sample (*3*) that was mounted in water. The radiation spot diameter on the sample with sharp edges was varied in the course of the experiments from 1 to 2 mm.

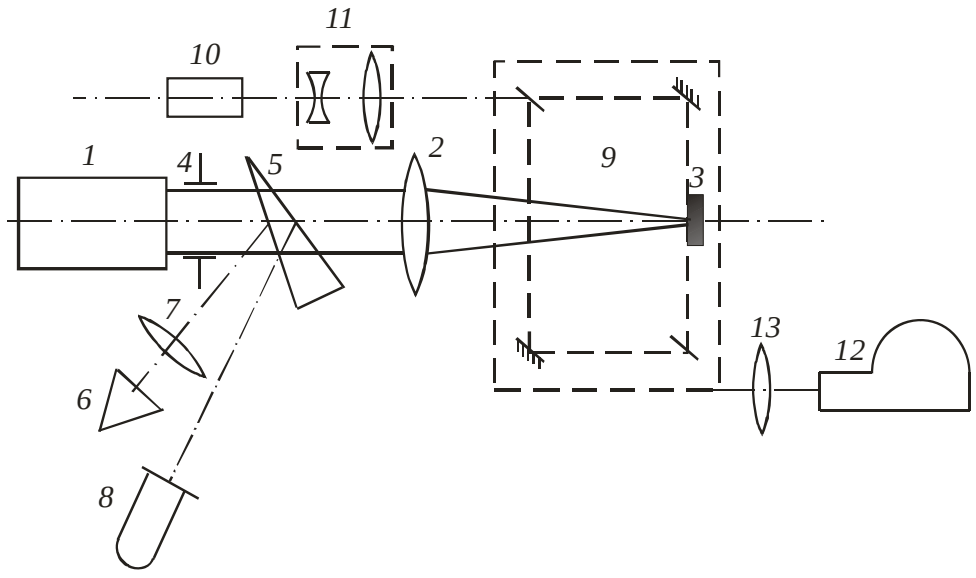

Fig. 1. Schematic diagram of the experimental setup

http://dx.doi.org/10.18720/MPM.4112019_15

From the front face of the glass wedge (*5*) a part (4 %) of laser radiation was directed into the IMO-2N energy meter (*6*), which entrance window was located in the focal plane of the lens (*7*). The laser pulse energy was varied from 5 to 60 J. The FEK-14 coaxial photodetector (*8*), the signal from which was coupled to the S8-13 oscilloscope, was used to record the temporal shape of the laser pulse. To study the spatial and temporal evolution of the laser plasma torch in the course of laser radiation action on a sample, we used the method of high-speed holographic motion-picture recording [1]. The sample (*3*) was placed in one of the arms of Mach–Zehnder interferometer (*9*), which was illuminated with the radiation of the ruby laser (*10*) (l = 0.694 μm) operating in the free oscillation regime. The pulse duration of the radiation amounted to 400 ms. The transverse mode selection in the probing laser was accomplished using the aperture placed in the cavity, and the longitudinal mode selection was provided by the Fabry–Perot cavity standard used as the output mirror.

The probing radiation after the collimator (*11*) was a parallel light beam with the diameter up to 3 cm, which allowed observation of the steam-plasma cloud development. The interferometer was attached to the SFR-1M high-speed recording camera (*12*), in which the film plane was conjugate with the meridian section of the laser beam, acting on the sample, by means of the objective (*13*).

The high-speed camera operated in a time magnifier regime. The setup described allowed recording the time-resolved holograms of the focused image of a laser plasma torch. Separate holographic frames provided temporal resolution no worse than 0.8 μc (the single frame exposure time) and the spatial resolution in the object field ~ 50 μm. The diffraction efficiency of the holograms allowed one to reconstruct and record interference and shadow pictures of the studied process under the stationary conditions.

The experimental results have shown that the crater topography obtained on laser treating of a lead sample in water (Fig. 2) differs considerably from that of obtained on laser treating of the same sample in air under normal conditions (pressure ~ 10^5 Pa, Fig. 3).

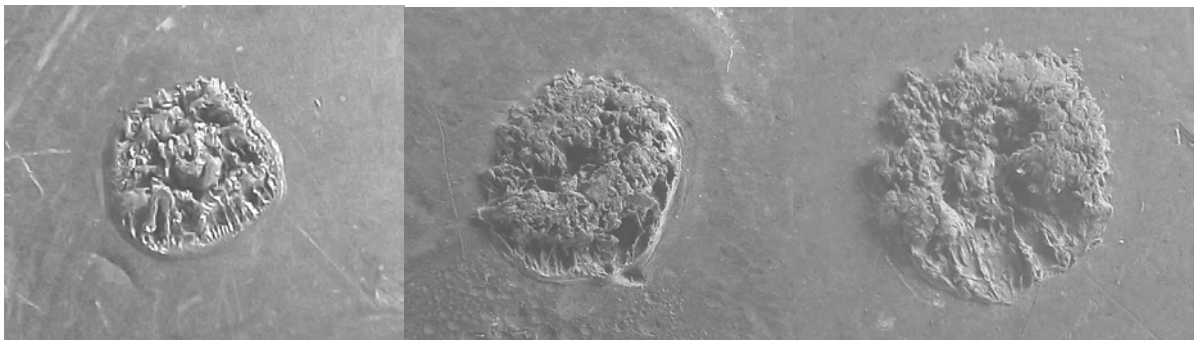

a). b). c).

Fig. 2. Craters obtained in water after treating a lead sample by laser pulses with energy 10 J (a), 20 J (b), 40 J (c)

To study the shape of crater that appears on the plate, we used the fringe projection method [2], which in the present case appeared to be more efficient than holographic methods of surface relief imaging and the stereo-photogrammetric method, since, already at the stage of fringe projecting, it allowed obtaining a picture with controllable measurement sensitivity and sufficiently good visibility of a relative fringe displacement. The first was set by changing the projected fringeperiod; the good visibility was provided by changing the illumination angle to the studied surface till removing the light flares from the crater surface. The present method is thoroughly described and successfully used in Ref. [3]. The crater surface obtained in water after treating of the lead sample by laser pulses is foamed; the macroscopic alveolus is practically absent (Fig. 2). The crater obtained in air after treating of lead sample by laser

pulse has an alveolus with a plane surface (Fig. 3a). The crater topography (Fig. 3b) is determined by distribution of light energy density over the transverse cross-section of the laser beam [4].The shadow pictures obtained at different time are represented in Fig. 4. Near the surface of irradiated sample, there appear steam and gas bubbles. At the first stage its form is spherical. A bubble rapidly grows (especially during the early stages).

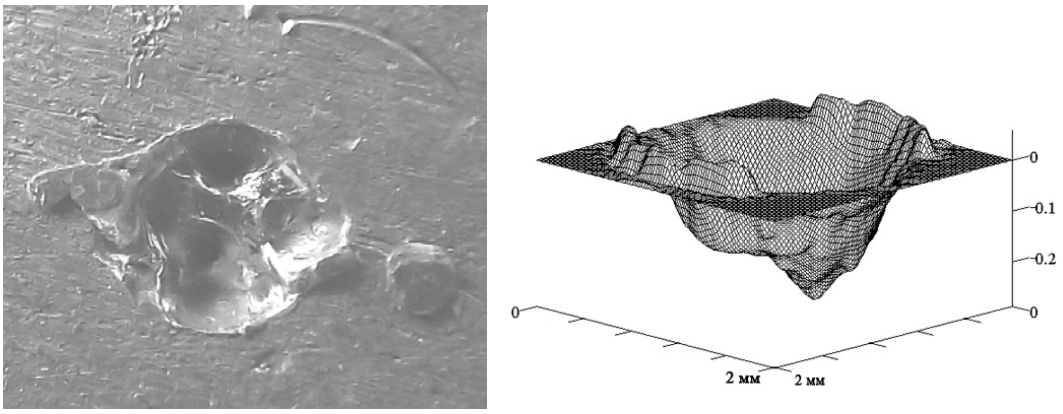

a) b)

Fig. 3. Crater obtained in air after treating of a lead sample by laser pulse with energy 40 J (a) and its topography (b)

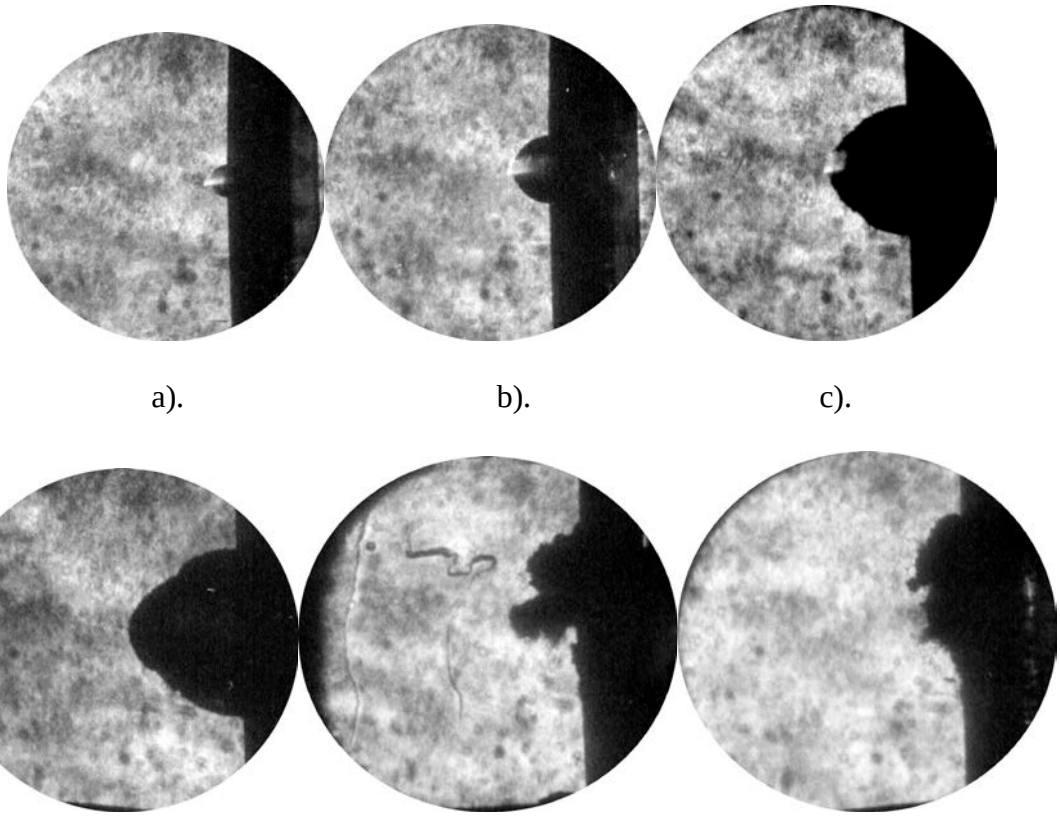

a). b). c).

d). e). f).

Fig.4. Shadow pictures of steam and plasma bubble obtained at 10 (a), 50 (b), 500 (c), 1200 (d), 2000 (e), 3000 (f) μc after the start of laser treating a lead sample

Figure 5 represents, defined from the shadow pictures, temporal dependences of the bubble radius and growth velocity.

Approximately in 500 μs after beginning the laser treating of the lead sample, the bubble form begins to change (Fig. 4c, d). After the cessation of laser irradiation (~ 1.2 ms) the bubble dimension stabilizes and only in ~ 1.5 ms starts its slow decay. It is important that the bubble form at this stage changes accidentally and it don't repeat oneself from one experiment to the other.

It should be mentioned that the metal drops, illuminated by laser radiation, were seen in the bubble and out of it at all the stages of laser treating. Both spectral analysis and X-ray analysis provided using devise ElvaX showed that a small amount of lead appears in the water after laser treating the lead sample because of nanoparticle gel formation.

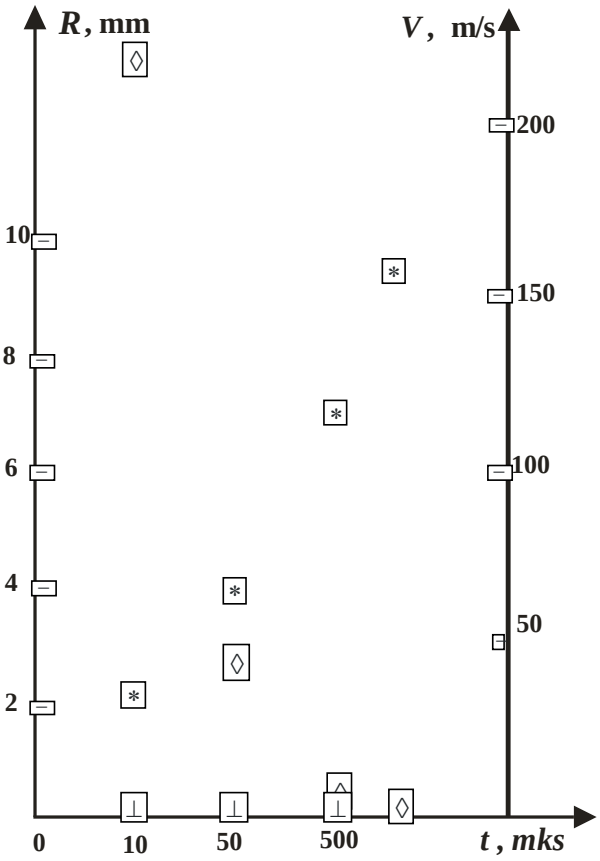

Fig. 5. Temporal dependences of the bubble radius (*) and its growth velocity (◊)

3.Discussion

During the treating of metal sample mounted in air by laser radiation with the parameters corresponding to our experiment [3] under normal condition (pressure ~ 10^5 Pa) dimension of generated plasma plume reached several centimeters. In the water shining zone of plasma plume has dimension ~ 1 mm; temperature on the plume board reaches ~ 7000 K [5]. The difference is explained by intensive heating and evaporation of water that leads to steam and gas bubble formation. There are two components inside the bubble: products of the irradiated sample erosion (lead steam) and water steam. The motion equations of these components are:

- Euler equations for each component

$$\rho_1 \frac{\partial \vec{V}}{\partial t} + \rho_1 \left(\vec{V} \cdot \nabla\right)\vec{V} = -\nabla p \ ,$$

$$\rho_2 \frac{\partial \vec{U}}{\partial t} + \rho_2 \left(\vec{U} \cdot \nabla\right)\vec{U} = -\nabla p \ ,$$

- Continuity equations for each component

$$\frac{\partial \rho_1}{\partial t} + div\left(\rho_1 \vec{V}\right) = A(t)\delta\left(r - r_0\right), \ \frac{\partial \rho_2}{\partial t} + div\left(\rho_2 \vec{U}\right) = B(t)\delta\left(r - r_b\right),$$

- State equations for each component

$$p = p_1 + p_2 \,, \ p_1 = \rho_1 \frac{R_u T}{\mu_1}, \ p_2 = \rho_2 \frac{R_u T}{\mu_2},$$

- Heat and mass transfer equation

$$\left(\rho_1 c_{p1} + \rho_2 c_{p2}\right)\frac{\partial T}{\partial t} + \left(\rho_1 c_{p1} \vec{V} + \rho_2 c_{p2} \vec{U}\right) \cdot \nabla T = div\left((\alpha_1 + \alpha_2)\nabla T\right).$$

Here ρ_1 is the ablation products gas density, ρ_2 is the water steam density, $\vec{V}$ is the ablation products gas velocity, $\vec{U}$ is the water steam velocity, $A(t)$ is the power density of the ablation products source (its temporal form repeats the temporal form of the laser pulse shown in Figure 6), $r = r_0$ is the equation of the plasma plume board, $B(t)$ is the power density of a water steam source, p_1 is the ablation products partial pressure, p_2 is the water steam partial pressure, T is the system temperature, μ_1 is the ablation products molar mass, μ_2 is the water steam molar mass, R_u is the universal gas constant, c_{p1} is the ablation products specific heat capacity under constant pressure, c_{p2} is the water steam specific heat capacity under constant pressure, α_1 is the ablation products heat conductivity, α_2 is the water steam heat conductivity, h is the specific heat of water evaporation, D is a coefficient, p_a is the atmospheric pressure, M is the mass of the water in the cuvette, S_b is the bubble surface area, a is the bubble surface acceleration, $B(t) = D\dfrac{(\alpha_1 + \alpha_2)|\nabla T|}{h}\Big|r = r_b$.

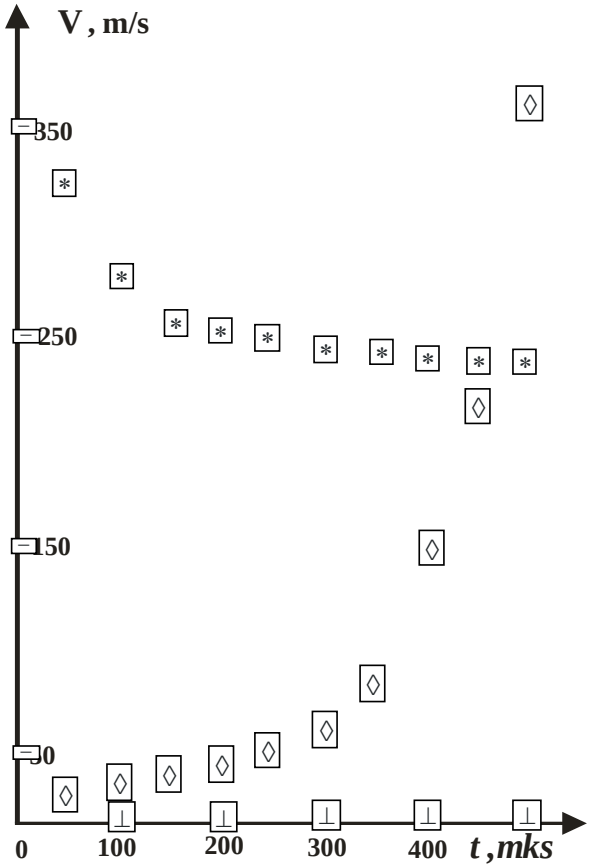

Fig. 6. Temporal dependences of ablation products (*) and water steam (◊) velocities at the distance $r = \Delta r / 2$ from the bubble surface

The solution of the equation system with the boundary conditions

$T\big|\, r = r_0 = 7000K$, $T\big|\, r = r_b = 373K$, $V_n\big|\, z=0 = U_n\big|\, z=0 = 0$, $(p - p_a)\big|\, r = r_b = a \cdot M / S_b$

gives the following results.A small plasma plume emits a stream of hot ablation products in the opposite direction with respect to the laser beam. At the first stage ($t \le 10\ \mu c$) because of the high density and temperature ($T\big|\, r = r_0 = 7000K$) of erosion products, plasma motion is similar to that of observed in air. Here r_0 is plasma plume near a treated surface radius. The motion of erosion products is supersonic and practically one-dimensional (radial). The erosion products cool evaporating water. The velocity of bubble board motion is also supersonic. An intensive flow of the lead drops from the erosion zone is typical for this stage.

At the second stage ($10\ \mu c \le t \le 50\ \mu c$) the erosion products motion is also supersonic, but at this stage the water steam mass is considerably greater than the mass of erosion products in the bubble. The velocity of bubble board $\vec{U}_b$ is under-sonic, the velocity of water steam motion $\vec{U}$ is also under-sonic and considerably less $\vec{U}_b$, but $|\vec{U}|$ increases. The motion

of two-component (lead and water steam) system is radial. A part of evaporated products of erosion leave the bubble and form the water and lead nanoparticle gel.

At the third stage ($50\ \mu c \le t \le 500\ \mu c$) the velocities of all bubble components become under-sonic. The system of bubble motion equations for the components can be transformed into a linear one, being solved analytically. For instance, temperature in the bubble

$$T(r,t) = \frac{4T_0\ \Delta r}{\pi^3} \sum_{n=1}^{\infty} \frac{(1-(-1)^n)}{n^3} \exp\left(-\left(\frac{\pi n}{\Delta r}\right) A\, t\right) \frac{\sin\left(\frac{\pi n}{\Delta r} r\right)}{r}.$$

Here $T_0 = T\,|\,r = r_0$, $\Delta r = r_b - r_0$, $A = \frac{\alpha_1 + \alpha_2}{\rho_{01} c_{p1} + \rho_{20} c_{p2}}$, $A = \frac{\alpha_1 + \alpha_2}{\rho_{01} c_{p1} + \rho_{20} c_{p2}}$,

$\rho_{01} = \frac{\mu_1\ p\,|\,r = r_b}{R_u\ T\,|\,r = r_b}$, $\rho_{02} = \frac{\mu_2\ p\,|\,r = r_b}{R_u\ T\,|\,r = r_b}$.

Figure 6 represents the temporal dependences of ablation products and water steam velocities at the distance $r = \Delta r / 2$ from the bubble surface. It is considerable that at the end of this stage of process a stream of water steam becomes supersonic.

At the forth stage ($t \ge 500\ \mu c$) the water steam motion becomes not one-dimensional (radial). Reaching a bubble board the water steam stream moves transversal to the bubble board ofa sample, reaches it, moves along the sample to its centrum, reaches a plume, heats and moves opposite to a laser beam together with erosion products. So the stream of water steam moving along the sample to its centrum, don't avoid the melted metal flow out of the crater and froths it. In the contact zone of "direct" and "reverse" streams there appear vortexes. The vortexes exist among all bubble. This is the reason of incidental decay of the steam and gas bubble.

4. Conclusion

The investigations have showed that substantial difference in the forms of crater surfaces developed as a result of processing the identical targets, being in water or air, by laser pulses with the identical parameters are determined by principally different character of plasma and steam and gas mixture flow in the mentioned cases.

Acknowledgements. *No external funding was received for this study.*

References

[1] Ivanov AY, Nedolugov VI. Temporal characteristics of acoustic waves appearing when a laser pulse interacts with a metal surface. *Sov. J. Quantum Electronics*. 1989;19(4): 523-525.
[2] West CM. *Holographic Interferometry*. New York: John Wiley &Sons; 1979.
[3] Vasil'ev SV, Ivanov AY, Lyalikov AM. Topography of a crater formed by the action of a laser pulse on the surface of a metal. *Sov. J. Quantum Elelctronics*. 1995;25(8): 799-803.
[4] Bosak NA, Vasil'ev SV, Ivanov AY, Min'ko LY, Nedolugov VI, Chumakov AN. Characteristic features of the formation of a crater on the surface of a metal irradiated with repeated laser pulses. *Quantum Elelctronics*. 1999;29(4): 351-354.
[5] Tarasenko NN, Butsen AV, Tarasenko NV, Pankov VV. Laser treatment of nanoparticles in liquids: modification of structure and composition. In: Astashynski VM, Burakov VS, Filatova II. (eds.) *VII International Conference "Plasma Physics and Plasma Technology". Contributed papers. Volume 2. Minsk, Belarus, September 17–21, 2012*. Minsk: Kovcheg; 2012. p.479-482.